

# UC Irvine

## UC Irvine Previously Published Works

### Title

Contrast-to-Noise Ratio Optimization in Coronary Computed Tomography Angiography: Validation in a Swine Model

### Permalink

<https://escholarship.org/uc/item/0723k0q0>

### Journal

Academic Radiology, 26(6)

### ISSN

1076-6332

### Authors

Hubbard, Logan  
Malkasian, Shant  
Zhao, Yixiao  
[et al.](#)

### Publication Date

2019-06-01

### DOI

10.1016/j.acra.2018.06.026

Peer reviewed



Published in final edited form as:

*Acad Radiol.* 2019 June ; 26(6): e115–e125. doi:10.1016/j.acra.2018.06.026.

## Contrast-to-Noise Ratio Optimization in Coronary Computed Tomography Angiography: Validation in a Swine Model

Logan Hubbard, MS, Shant Malkasian, BS, Yixiao Zhao, MS, Pablo Abbona, MD, Sabeel Molloy, PhD

Department of Radiological Sciences, Medical Sciences I, B-140, University of California, Irvine, Irvine, CA 92697.

### Abstract

**Rationale and Objectives:** The accuracy of coronary computed tomography (CT) angiography depends upon the degree of coronary enhancement as compared to the background noise. Unfortunately, coronary contrast-to-noise ratio (CNR) optimization is difficult on a patient-specific basis. Hence, the objective of this study was to validate a new combined diluted test bolus and CT angiography protocol for improved coronary enhancement and CNR.

**Materials and Methods:** The combined diluted test bolus and CT angiography protocol was validated in six swine ( $28.9 \pm 2.7$  kg). Specifically, the aortic and coronary enhancement and CNR of a standard CT angiography protocol, and a new combined diluted test bolus and CT angiography protocol were compared to a reference retrospective CT angiography protocol. Comparisons for all data were made using box plots, *t* tests, regression, Bland–Altman, root-mean-square error and deviation, as well as Lin's concordance correlation.

**Results:** The combined diluted test bolus and CT angiography protocol was found to improve aortic and coronary enhancement by 26% and 13%, respectively, as compared to the standard CT angiography protocol. More importantly, the combined protocol was found to improve aortic and coronary CNR by 29% and 20%, respectively, as compared to the standard protocol.

**Conclusion:** A new combined diluted test bolus and CT angiography protocol was shown to improve coronary enhancement and CNR as compared to an existing standard CT angiography protocol.

### Keywords

Contrast-to-noise ratio; Coronary artery disease; Computed tomography angiography; Test bolus; Time to peak

## INTRODUCTION

Coronary computed tomography (CT) angiography is a powerful tool for noninvasive diagnosis of coronary artery disease. However, the accuracy of CT angiography depends

---

**Address correspondence to:** S.M. symolloi@uci.edu.

**Disclosures:** The authors do not have any conflicts of interest to disclose.

upon the degree of coronary enhancement and contrast-to-noise ratio (CNR) (1,2). Fortunately, automatic exposure control can be used to optimize image noise (3,4), whereas dynamic bolus tracking can be used to trigger CT angiography acquisition (5,6). Unfortunately, patient-specific hemodynamic variability renders dynamic bolus tracking unreliable in coronary enhancement optimization (7-9). Hence, small-volume test bolus injections (10–15 mL) are often used prior to CT angiography acquisition to predict the time-to-peak enhancement (8,10). However, the time-to-peak predictions of such test bolus techniques are also known to be highly variable (11-13); hence, the problem of patient-specific coronary enhancement and CNR optimization remains largely unsolved (7,8,11,14-16).

Fortunately, recent work suggests that the peak enhancement of large-volume diluted test bolus injections is highly predictive of CT angiography peak enhancement (17). Moreover, additional work suggests that bolus injection volume is most predictive of bolus width (18,19), where the time-to-peak enhancement occurs at one-half the bolus width. Hence, a diluted test bolus of equivalent volume to that of a CT angiography bolus has the potential to accurately predict the time-to-peak enhancement necessary for patient-specific CT angiography optimization. Therefore, the purpose of this study was to validate a new combined diluted test bolus and CT angiography protocol for improved coronary enhancement and CNR. The central hypothesis was that a diluted test bolus can be used prior to CT angiography acquisition to accurately predict the time to peak necessary for optimal coronary enhancement and CNR.

## METHODS

### General Methods

The study was approved by the Animal Care Committee and was performed in agreement with the “Position of the American Heart Association on Research Animal Use.” Six male Yorkshire swine ( $28.9 \pm 2.7$  kg) were used, with two experimental aims of interest. When possible, repeat measurements were made, with both experimental aims completed successfully. All image data were acquired between May 2017 and July 2017, and were retrospectively analyzed between July 2017 and November 2017.

### Animal Preparation

Anesthesia was induced with telazol (4.4 mg/kg), ketamine (2.2 mg/kg), and xylazine (2.2 mg/kg), and was maintained with 1.5%–2.5% isoflurane (Highland Medical Equipment, Temecula, CA and Baxter, Deerfield, IL). Sheaths were placed (5Fr, AVANTI, Cordis Corporation, Miami Lakes, FL) in each femoral vein and were used for drug, fluid, and contrast material administration.

### Prediction of Time-To-Peak Enhancement

For each animal, standard undiluted and diluted test bolus injection protocols were performed followed by dynamic imaging and analysis to determine which test bolus was most predictive of a reference CT angiography bolus time-to-peak enhancement. When possible, repeat measurements were also made in six swine, yielding a total of 14

measurements for the standard test bolus protocol analysis, and a total of 12 measurements for the diluted test bolus protocol analysis.

**Standard Test Bolus Protocol**—For the standard bolus protocol, 10 mL of contrast material (Iovue 370, Bracco Diagnostics, Princeton, NJ) was injected (5 mL/s, Empower CTA, Acist Medical Systems, Eden Prairie, MN) followed by saline chaser (0.5 mL/kg) at the same rate. Volume scans were then acquired (Aquilion One, Toshiba America Medical Systems, Tustin, CA) over 20 seconds to capture the time–attenuation curve, as shown in Figure 1a.

**Diluted Test Bolus Protocol**—For the diluted bolus protocol, 10 mL of contrast material was diluted in saline (1 mL/kg) and was injected (5 mL/s) followed by a saline chaser (0.5 mL/kg) at the same rate. Volume scans were then acquired over 20 seconds to capture the time–attenuation curve, as shown in Figure 1b.

**Reference CT Angiography Bolus Protocol**—For the reference bolus protocol, 1 mL/kg of contrast material, was injected (5 mL/s) followed by a saline chaser (0.5 mL/kg) at the same rate. Volume scans were then acquired over 20 seconds to capture the reference CT angiography bolus time–attenuation curve, as shown in Figure 1c.

**CT Imaging**—All dynamic imaging protocols were electrocardiogram (ECG) gated and were performed at 100 kVp and 200 mA with  $320 \times 0.5$  mm collimation and 16 cm of craniocaudal coverage. Additionally, a 10-minute delay was employed after each protocol to allow for adequate clearance of contrast material from the blood pool prior to initiating the next protocol. After imaging was complete, all volume scans were retrospectively reconstructed from full projection data at 75% of the R–R interval using an FC03 kernel and a reconstruction voxel size of  $0.43 \times 0.43 \times 0.50$  mm.

**Image Processing**—For each series of acquisitions, the volume scan with peak aortic enhancement was selected from the reference bolus volume scans, and all test bolus and reference bolus volume scans were deformably registered to that peak enhancement volume scan to minimize motion artifacts (20). The aorta was then segmented semiautomatically through threshold-based region growing (Vitrea fX version 6.0, Vital Images, Inc., Minnetonka, MN), producing a vascular volume of interest. The vascular volume of interest was then radially eroded by two voxels to eliminate partial volume artifact, yielding the central luminal volume of the aorta. Using that central luminal volume, time–attenuation curves for the test bolus and reference bolus data were produced by computing the average Hounsfield unit within that luminal volume over time. Time-to-peak enhancement data for each protocol were then extracted with a gamma-variate fit function (MatLab 2013a, MathWorks, Natick, MA). The image processing scheme is summarized in Figure 2a.

### Optimization of Enhancement and CNR

For each animal, a standard CT angiography protocol was performed along with a combined diluted test bolus and CT angiography protocol. In each case, the CT dose index ( $CTDI_{VOL}^{32}$ ) and dose-length product (DLP) were also recorded. The peak enhancement and CNR for the

left anterior descending (LAD), left circumflex (LCx), and right coronary artery (RCA) for the standard and combined protocols were then compared to corresponding data from a reference retrospective CT angiography protocol. When possible, repeat measurements were also made in six swine, yielding a total of 10 measurements for the peak enhancement and CNR analysis.

**Standard CT Angiography Protocol**—For the standard CT protocol, 1 mL/kg of contrast material was injected (5 mL/s) followed by a saline chaser (0.5 mL/kg) at the same rate. Dynamic bolus tracking was used (Sure-Start, Aquilion One, Toshiba America Medical Systems, Tustin, CA), and a CT angiogram was acquired automatically using a standard clinical protocol with a fixed time delay of 4 seconds after threshold-based triggering at 180 Hounsfield units in the aorta, as shown in Figure 3a.

**Combined Diluted Test Bolus and CT Angiography Protocol**—For the combined CT protocol, 10 mL of contrast material was diluted in saline (1 mL/kg) and was injected (5 mL/s) followed by a saline chaser (0.5 mL/kg) at the same rate. A 2 mm slab CINE scanning was then performed in 1.5-second intervals over 20 seconds, and the time-to-peak aortic enhancement was derived. The CT angiography protocol was then manually updated to incorporate the measured time to peak. Of contrast material, 1 mL/kg was then injected (5 mL/s) followed by a saline chaser (0.5 mL/kg) at the same rate. Dynamic bolus tracking was again used, but this time the CT angiogram was acquired using the new time-to-peak delay after threshold-based triggering at 180 Hounsfield units in the aorta, as shown in Figure 3b.

**Reference Retrospective CT Angiography Protocol**—For the reference CT protocol, 1 mL/kg of contrast material was injected (5 mL/s) followed by a saline chaser (0.5 mL/kg) at the same rate. Volume scans were then acquired over 20 seconds to capture the reference retrospective CT angiography time–attenuation curve, as shown in Figure 3c.

**CT Imaging**—All dynamic imaging protocols were ECG gated and were performed at 100 kVp and 200 mA, where all bolus tracking images had a collimation of  $1 \times 2.0$  mm and all volume scans had a collimation of  $320 \times 0.50$  mm. Additionally, a 10-minute delay was employed after each protocol to allow for adequate clearance of contrast material from the blood pool prior to initiating the next protocol. After imaging was complete, all bolus tracking images and volume scans were retrospectively reconstructed from full projection data at 75% of the R–R interval using an FC03 kernel and a reconstruction voxel size of  $0.43 \times 0.43 \times 2.0$  mm and  $0.43 \times 0.43 \times 0.50$  mm, respectively.

**Image Processing**—For each series of acquisitions, the volume scan with peak aortic enhancement was selected from the reference retrospective volume scans, and all CT angiograms and reference retrospective volume scans were deformably registered to that peak enhancement volume scan to minimize motion artifacts (20). The aorta, LAD, LCx, and RCA were then segmented semiautomatically through threshold-based region growing (Vitreax fX version 6.0, Vital Images, Inc., Minnetonka, MN), producing four separate vascular volumes of interest. Each vascular volume of interest was then radially eroded by two voxels to eliminate partial volume artifact, yielding the central luminal volume of the aorta, LAD, LCx, and RCA. Peak enhancement and CNR data were then computed within

each central luminal volume for each protocol, where CNR was defined as the attenuation difference between each central luminal volume and the left ventricular myocardium, divided by the image noise. The image processing scheme is summarized in Figure 2b.

### Statistical Approach

First, the accuracy and precision of both test bolus protocols in prediction of reference bolus time-to-peak aortic enhancement were assessed using regression, Bland–Altman, root-mean-square error, root-mean-square deviation, and Lin's concordance correlation coefficient (21). Box plots were generated, and paired sample  $t$ -tests were performed to determine if the time-to-peak enhancement of each protocol was significantly different from the reference protocol ( $p < 0.05$ ). Next, the accuracy and precision of both CT angiography protocols in prediction of a reference retrospective CT angiography protocol's peak enhancement and CNR were assessed using regression, Bland–Altman, root-mean-square error, root-mean-square deviation, and Lin's concordance correlation coefficient (21). Box plots were again generated, and paired sample  $t$  tests were again performed to determine if the peak enhancement and CNR of each protocol were significantly different from the reference protocol ( $p < 0.05$ ). Statistical software was used for all analysis (MatLab 2013a, MathWorks, Natick, MA; PS, version 3.0, Vanderbilt University, Nashville, TN; SPSS, version 22, IBM Corporation, Armonk, NY).

## RESULTS

### Prediction of Time-To-Peak Enhancement

The heart rate and mean arterial pressure of the swine were  $88 \pm 13$  beats/min and  $75 \pm 19$  mmHg, respectively. The test bolus and reference CT angiography bolus enhancement curves are displayed in Figure 4a, whereas the test bolus and reference CT angiography bolus time-to-peak data box plots are shown in Figure 4b. On average, the time-to-peak data for the standard test bolus and diluted test bolus were  $4.9 \pm 1.5$  ( $p = 0.00$ ) and  $6.4 \pm 1.6$  ( $p = 0.88$ ) seconds, respectively, whereas the time-to-peak data for the reference CT angiography bolus was  $6.2 \pm 1.6$  seconds. Furthermore, the time-to-peak data for the standard test bolus ( $TTP_{STB}$ ) and reference CT angiography bolus ( $TTP_{REF}$ ) were related with a Pearson's correlation of  $r = 0.78$  and a concordance correlation of  $\rho = 0.57$ , as shown in Figure 4c, with corresponding Bland–Altman analysis displayed in Figure 4d. Finally, the time-to-peak data for the diluted test bolus ( $TTP_{DTB}$ ) and reference CT angiography bolus ( $TTP_{REF}$ ) were related with a Pearson's correlation of  $r = 0.97$  and a concordance correlation of  $\rho = 0.96$ , as shown in Figure 4e, with corresponding Bland–Altman analysis displayed in Figure 4f.

### Optimization of Enhancement and CNR

The  $CTDI_{VOL}^{32}$  and DLP of the standard CT angiography protocol were 4.6 mGy and 73.6 mGy●cm, respectively. The  $CTDI_{VOL}^{32}$  and DLP of the diluted test bolus alone were 59.8 mGy and 12.0 mGy●cm, respectively. In combination, the  $CTDI_{VOL}^{32}$  and DLP of the combined diluted test bolus and CT angiography protocol were 64.4 mGy and 85.6 mGy●cm, respectively. Box plots for the standard, combined, and reference retrospective

CT angiography protocol peak enhancement and CNR data are shown in Figure 5a and b, respectively, with corresponding paired sample *t*-test data also shown in Table 1.

Furthermore, for the standard CT angiography protocol, the peak enhancement data ( $PEAK_{STAN}$ ) in both the aorta and coronaries were related to the reference retrospective CT angiography peak enhancement data with a Pearson's correlation of  $r = 0.83$  and a concordance correlation of  $\rho = 0.76$ , as shown in Figure 6a and Table 2, with corresponding Bland–Altman analysis displayed in Figure 6b. The CNR data ( $CNR_{STAN}$ ) in both the aorta and coronaries were also related to the reference retrospective CT angiography CNR data ( $CNR_{REF}$ ) with a Pearson's correlation of  $r = 0.90$  and a concordance correlation of  $\rho = 0.84$ , as shown in Figure 7a and Table 2, with corresponding Bland–Altman analysis also displayed in Figure 7b.

Finally, for the combined diluted test bolus and CT angiography protocol, the peak enhancement data ( $PEAK_{COMB}$ ) in both the aorta and coronaries were related to the reference retrospective CT angiography peak enhancement data ( $PEAK_{REF}$ ) with a Pearson's correlation of  $r = 0.96$  and a concordance correlation of  $\rho = 0.96$ , as shown in Figure 6c and Table 2, with corresponding Bland–Altman analysis displayed in Figure 6d. The CNR data ( $CNR_{COMB}$ ) in both the aorta and coronaries were also related to the reference retrospective CT angiography CNR data ( $CNR_{REF}$ ) with a Pearson's correlation of  $r = 0.97$  and a concordance correlation of  $\rho = 0.97$ , as shown in Figure 7c and Table 2, with corresponding Bland–Altman analysis displayed in Figure 7d. Qualitative multiplanar reformations of the LAD for the standard, combined, and reference retrospective CT angiography protocols are shown in Figure 5c.

## DISCUSSION

In this study, standard undiluted and diluted test bolus injection protocols were first performed followed by dynamic imaging and analysis to determine which test bolus was most predictive of reference CT angiography bolus time-to-peak enhancement. A standard CT angiography protocol was then performed along with a combined diluted test bolus and CT angiography protocol, and the peak enhancement and CNR of the LAD, LCx, and RCA for both protocols were then compared to a reference retrospective CT angiography protocol.

The results indicate that a diluted test bolus can be used to accurately predict the time-to-peak enhancement of a CT angiography bolus. However, a standard test bolus was shown to underestimate the time-to-peak enhancement by more than 20%. Furthermore, the diluted test bolus performed better than the standard test bolus in time-to-peak enhancement prediction, demonstrating higher concordance correlation (21) and negligible bias, as compared to the reference CT angiography bolus. Such findings indicate that the enhancement of a diluted test bolus does, in fact, parallel that of a CT angiography bolus, independent of cardiac output.

Moreover, the combined diluted test bolus and CT angiography protocol was found to improve peak aortic and coronary enhancement and CNR by 26%, 13%, 29%, and 20%, respectively, as compared to the standard CT angiography protocol, while only increasing

the DLP by 16%. Additionally, the combined diluted test bolus and CT angiography protocol demonstrated better concordance correlation (21) and less bias than the standard CT angiography protocol, as compared to the reference retrospective CT angiography protocol. Such findings indicate that a diluted test bolus can, in fact, be used to significantly improve peak enhancement and CNR through accurate prediction of the time to peak necessary for optimal acquisition of the CT angiogram.

Overall, the findings of this study agree with the findings of others regarding optimization of CT angiography. Specifically, the limitations of the standard test bolus in prediction of time-to-peak enhancement agree well with the findings of van Hoe et al. and Kaatee et al., where poor-to-moderate correlation was found with the actual time to peak of the CT angiography bolus (12,13). Additionally, with respect to using a test bolus versus dynamic bolus tracking for CT angiography, Nakajima et al. and Rodrigues et al. also found better peak enhancement and CNR when using a test bolus with a patient-specific time delay as compared to dynamic bolus tracking with a fixed time delay (10,22). Nevertheless, Nakaura et al. and Platt et al. found no such improvements (8,14), but this difference is likely attributed to the fact that a standard test bolus has a different time–attenuation curve as compared to a CT angiography bolus.

To improve test bolus reliability, Masuda et al. evaluated the performance of a diluted and standard test bolus in prediction of peak enhancement of CT angiography in the aorta (17). Interestingly, they found that peak enhancement for a diluted test bolus was strongly predictive of peak enhancement for CT angiography, whereas peak enhancement for a standard test bolus was not ( $r = 0.72$  vs.  $r = 0.36$ ). Such findings are further explained by work done by Garcia et al. and Han et al., where injection volume was found to be most predictive of bolus width (18,19). That being said, the work of Masuda et al. remained limited to aortic peak enhancement prediction alone. Hence, our study focuses instead on the ability of a diluted test bolus to accurately predict the time-to-peak enhancement of a CT angiography bolus. Moreover, we use those time-to-peak predictions to improve the peak enhancement and CNR of CT angiography in the aorta, LAD, LCx, and RCA.

However, this study is not without limitations. First, the study was performed on a small number of healthy swine, reducing the power of the study while also limiting assessment of CT angiography quality to coronary enhancement and CNR alone. Hence, validation in a human cohort using CT angiography quality assessment metrics such as CNR, coronary length and number of side branches, stenosis severity, and plaque volume is still necessary (23). Additionally, while the standard, combined, and reference retrospective CT angiography protocols did employ a mass-adjusted contrast volume (1 mL/kg), the test bolus protocols did not (10 mL). Consequently, the test bolus peak enhancement was higher than the 100–200 Hounsfield unit enhancement normally seen in human subjects (8,17), as central blood volume scales proportionally with mass (15,24). However, given the analogous relation between the diluted test bolus and standard CT angiography bolus geometries, variations in central blood volume should not impact the diluted test bolus's ability to predict the time-to-peak enhancement for CT angiography. Hence, 10 mL of contrast was used for the test bolus protocols, as 10–15 mL test bolus injections are used clinically (11).

That being said, the inability of the standard CT angiography protocol to compensate for large variations in cardiac output was likely compounded by the high heart rate and significant heart rate variability of the swine used within this study. However, as cardiac output is the product of both heart rate and stroke volume, coronary artery disease patients will still display variations in cardiac output, time-to-peak, and peak enhancement, regardless of beta blockade, due to known variations in stroke work (7,9). Hence, it is expected that a combined diluted test bolus and CT angiography protocol will still provide more clinical value than a standard CT angiography protocol alone, although further validation is necessary.

Despite the advantages of the combined diluted test bolus and CT angiography protocol, implementation of such a protocol may be clinically complex. Specifically, the combined protocol requires diluted contrast to be made, injected, and imaged prior to CT angiography; thus, adding time, contrast dose, and effective radiation dose per exam. That being said, exam time can be reduced using injector technology that is capable of co-injection of contrast and saline, i.e., dilution, prior to serial injection of contrast and saline (25). Moreover, given the time-to-peak, peak enhancement, and CNR gains afforded by using a diluted test bolus, it may be possible to reduce the total volume of contrast necessary for patient-specific CT angiography, while still maintaining adequate image quality. Finally, with respect to effective radiation dose, the advent of dynamic bolus tracking and iterative reconstruction techniques (26) ensures that the dose of a diluted test bolus is very small (DLP = 12 mGy·cm), as compared to the dose of CT angiography (DLP = 73.6 mGy·cm). Furthermore, there is additional potential to improve dynamic bolus tracking techniques, such that time-to-peak enhancement prediction may be performed without the need for a diluted test bolus, although further validation is necessary.

## CONCLUSION

The combined diluted test bolus and CT angiography protocol uses a low-dose diluted test bolus for time-to-peak enhancement prediction prior to CT angiography. Given the analogous relation between the diluted test bolus and CT angiography bolus, the combined protocol ensures that peak enhancement and CNR are always achieved, independent of central blood volume or cardiac output. In summary, the combined diluted test bolus and CT angiography protocol was retrospectively validated in a swine model and has the potential to improve enhancement and CNR for CT angiography through optimal image acquisition timing.

## Acknowledgments

**Funding:** This work was supported, in part, by the Department of Radiological Sciences at the University of California, Irvine and by the American Heart Association under award number 17CPRE33650059.

## Abbreviations

CCC	Lin's concordance correlation coefficient
CT	computed tomography

<b>CNR</b>	contrast-to-noise ratio
<b>DTB</b>	diluted test bolus
<b>ECG</b>	electrocardiogram
<b>LAD</b>	left anterior descending
<b>LCx</b>	left circumflex
<b>RCA</b>	right coronary artery
<b>RMSE</b>	root-mean-square error
<b>RMSD</b>	root-mean-square deviation
<b>TTP</b>	time to peak

## REFERENCES

1. Cademartiri F, Mollet NR, Lemos PA, et al. Higher intracoronary attenuation improves diagnostic accuracy in MDCT coronary angiography. *AJR Am J Roentgenol* 2006; 187:430–433. [PubMed: 16861548]
2. Cademartiri F, Mollet NR, van der Lugt A, et al. Intravenous contrast material administration at helical 16-detector row CT coronary angiography: effect of iodine concentration on vascular attenuation. *Radiology* 2005;236:661–665. [PubMed: 16040923]
3. Papadakis AE, Perisinakis K, Damilakis J. Automatic exposure control in CT: the effect of patient size, anatomical region and prescribed modulation strength on tube current and image quality. *Eur Radiol* 2014; 24:2520–2531. [PubMed: 25027840]
4. Ghoshhajra BB, Engel L- C, Károlyi M, et al. Cardiac computed tomography angiography with automatic tube potential selection: effects on radiation dose and image quality. *J Thorac Imaging* 2013; 28:40–48. [PubMed: 22847638]
5. Schweiger GD, Chang PJ, Brown BP. Optimizing contrast enhancement during helical CT of the liver: a comparison of two bolus tracking techniques. *AJR Am J Roentgenol* 1998; 171:1551–1558. [PubMed: 9843287]
6. Eisa F, Brauweiler R, Peetz A, et al. Optical tracking of contrast medium bolus to optimize bolus shape and timing in dynamic computed tomography. *Phys Med Biol* 2012; 57:173–182. [PubMed: 22155989]
7. Sakai S, Yabuuchi H, Chishaki A, et al. Effect of cardiac function on aortic peak time and peak enhancement during coronary CT angiography. *Eur J Radiol* 2010; 75:173–177. [PubMed: 19442467]
8. Nakaura T, Awai K, Yanaga Y, et al. Low-dose contrast protocol using the test bolus technique for 64-detector computed tomography coronary angiography. *Jpn J Radiol* 2011; 29:457–465. [PubMed: 21882087]
9. Bae KT, Heiken JP, Brink JA. Aortic and hepatic contrast medium enhancement at CT. Part II. Effect of reduced cardiac output in a porcine model. *Radiology* 1998; 207:657–662. [PubMed: 9609887]
10. Rodrigues JC, Mathias H, Negus IS, et al. Intravenous contrast medium administration at 128 multidetector row CT pulmonary angiography: bolus tracking versus test bolus and the implications for diagnostic quality and effective dose. *Clin Radiol* 2012; 67:1053–1060. [PubMed: 22520034]
11. Cademartiri F, van der Lugt A, Luccichenti G, et al. Parameters affecting bolus geometry in CTA: a review. *J Comput Assist Tomogr* 2002; 26:598–607. [PubMed: 12218827]
12. van Hoe L, Marchal G, Baert AL, et al. Determination of scan delay time in spiral CT-angiography: utility of a test bolus injection. *J Comput Assist Tomogr* 1995; 19:216–220. [PubMed: 7890844]

13. Kaatee R, Van Leeuwen MS, De Lange EE, et al. Spiral CT angiography of the renal arteries: should a scan delay based on a test bolus injection or a fixed scan delay be used to obtain maximum enhancement of the vessels? *J Comput Assist Tomogr* 1998; 22:541–547. [PubMed: 9676443]
14. Platt JF, Reige KA, Ellis JH. Aortic enhancement during abdominal CT angiography: correlation with test injections, flow rates, and patient demographics. *AJR Am J Roentgenol* 1999; 172:53–56. [PubMed: 9888738]
15. Bae KT, Seeck BA, Hildebolt CF, et al. Contrast enhancement in cardiovascular MDCT: effect of body weight, height, body surface area, body mass index, and obesity. *AJR Am J Roentgenol* 2008; 190:777–784. [PubMed: 18287452]
16. Nakaura T, Awai K, Yauaga Y, et al. Contrast injection protocols for coronary computed tomography angiography using a 64-detector scanner: comparison between patient weight-adjusted- and fixed iodine-dose protocols. *Invest Radiol* 2008; 43:512–519. [PubMed: 18580334]
17. Masuda T, Funama Y, Imada N, et al. Prediction of aortic enhancement on coronary CTA images using a test bolus of diluted contrast material. *Acad Radiol* 2014;21:1542–1546. [PubMed: 25442352]
18. Garcia P, Genin G, Bret PM, et al. Hepatic CT enhancement: effect of the rate and volume of contrast medium injection in an animal model. *Abdom Imaging* 1999; 24:597–603. [PubMed: 10525816]
19. Han JK, Kim AY, Lee KY, et al. Factors influencing vascular and hepatic enhancement at CT: experimental study on injection protocol using a canine model. *J Comput Assist Tomogr* 2000; 24:400–406. [PubMed: 10864075]
20. Modat M, Ridgway GR, Taylor ZA, et al. Fast free-form deformation using graphics processing units. *Comput Methods Programs Biomed* 2010; 98:278–284. [PubMed: 19818524]
21. Lin LI. A concordance correlation coefficient to evaluate reproducibility. *Biometrics* 1989; 45:255–268. [PubMed: 2720055]
22. Nakajima Y, Yoshimine T, Yoshida H, et al. Computerized tomography angiography of ruptured cerebral aneurysms: factors affecting time to maximum contrast concentration. *J Neurosurg* 1998; 88:663–669. [PubMed: 9525712]
23. Ferencik M, Nomura CH, Maurovich-Horvat P, et al. Quantitative parameters of image quality in 64-slice computed tomography angiography of the coronary arteries. *Eur J Radiol* 2006; 57:373–379. [PubMed: 16439091]
24. Bae KT. Intravenous contrast medium administration and scan timing at CT: considerations and approaches. *Radiology* 2010; 256:32–61. [PubMed: 20574084]
25. Indrajit IK, Sivasankar R, D'Souza J, et al. Pressure injectors for radiologists: a review and what is new. *Indian J Radiol Imaging* 2015; 25:2–10. [PubMed: 25709157]
26. Halliburton SS, Tanabe Y, Partovi S, et al. The role of advanced reconstruction algorithms in cardiac CT. *Cardiovasc Diagn Ther* 2017; 7:527–538. [PubMed: 29255694]

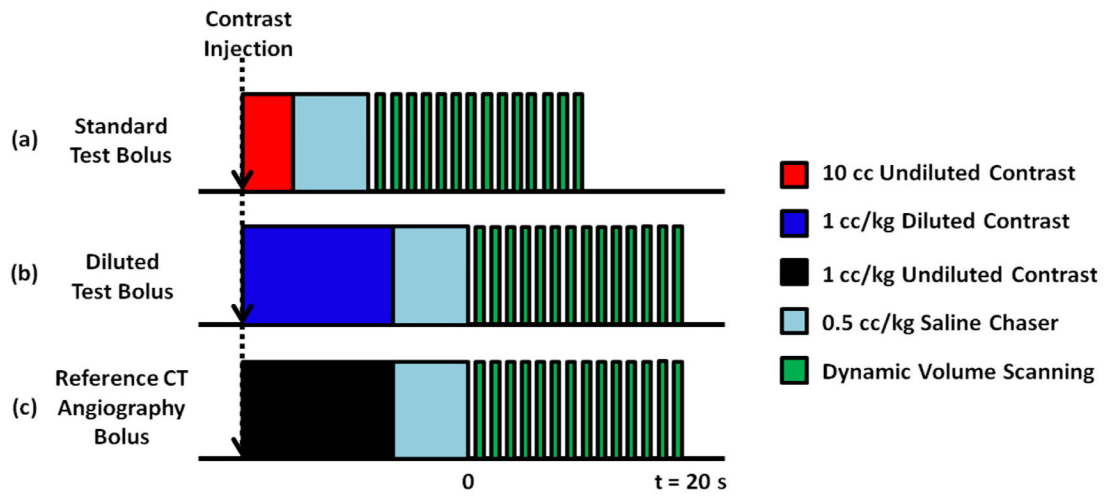


**Figure 1.** Standard, diluted, and reference CT angiography bolus injection protocol comparison. (a) Standard test bolus injection protocol, (b) diluted test bolus injection protocol, (c) reference CT angiography bolus injection protocol. All bolus injection protocols were followed by the same 20-second dynamic imaging protocol to completely capture each time–attenuation curve of interest for analysis. CT, computed tomography.

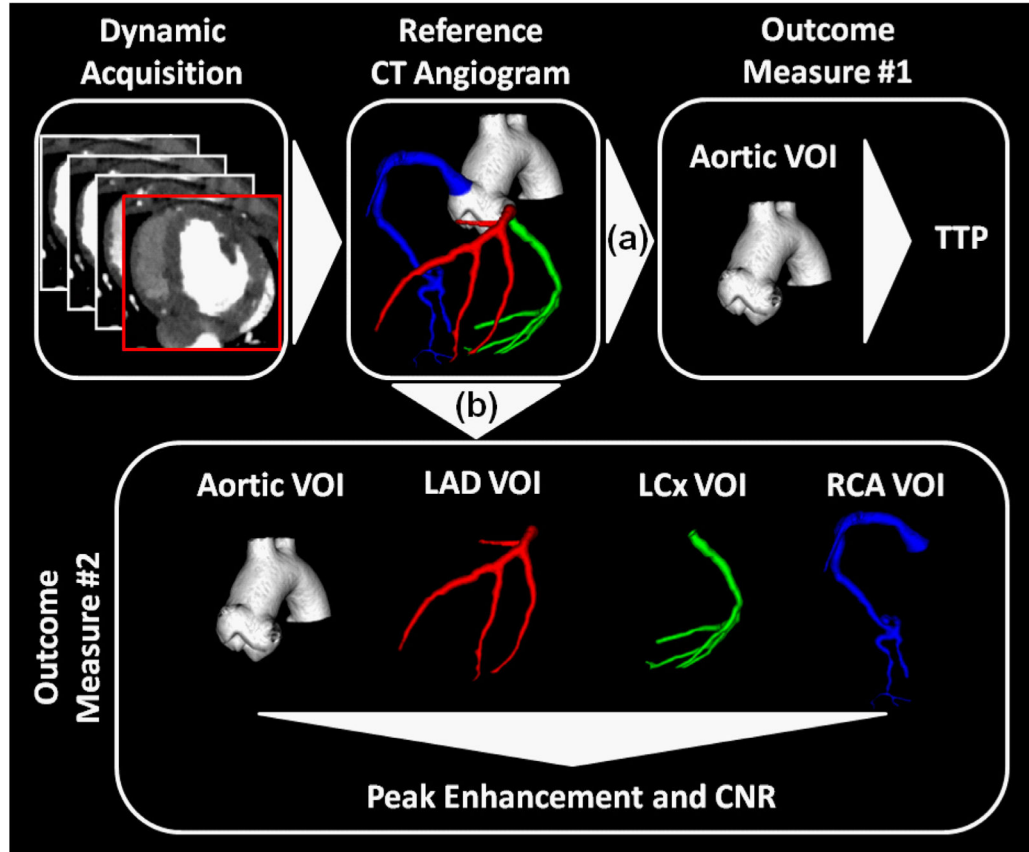


**Figure 2.** Image processing scheme. The peak enhancement volume scan was first selected from the reference computed tomography (CT) angiography bolus protocol data for vascular volume-of-interest (VOI) segmentation and postprocessing. **(a)** The aortic VOI was used to generate time–attenuation curves for the standard test bolus, diluted test bolus, and reference CT angiography bolus protocol data, and time-to-peak (TTP) enhancement data were then extracted in each case through automatic gamma-variate fitting. **(b)** The aortic VOI, left anterior descending (LAD) VOI, left circumflex (LCx) VOI, and right coronary artery (RCA) VOI were used to compute peak enhancement and contrast-to-noise ratio for both standard and combined CT angiography protocols, and all data were then compared to the reference retrospective CT angiography protocol data.

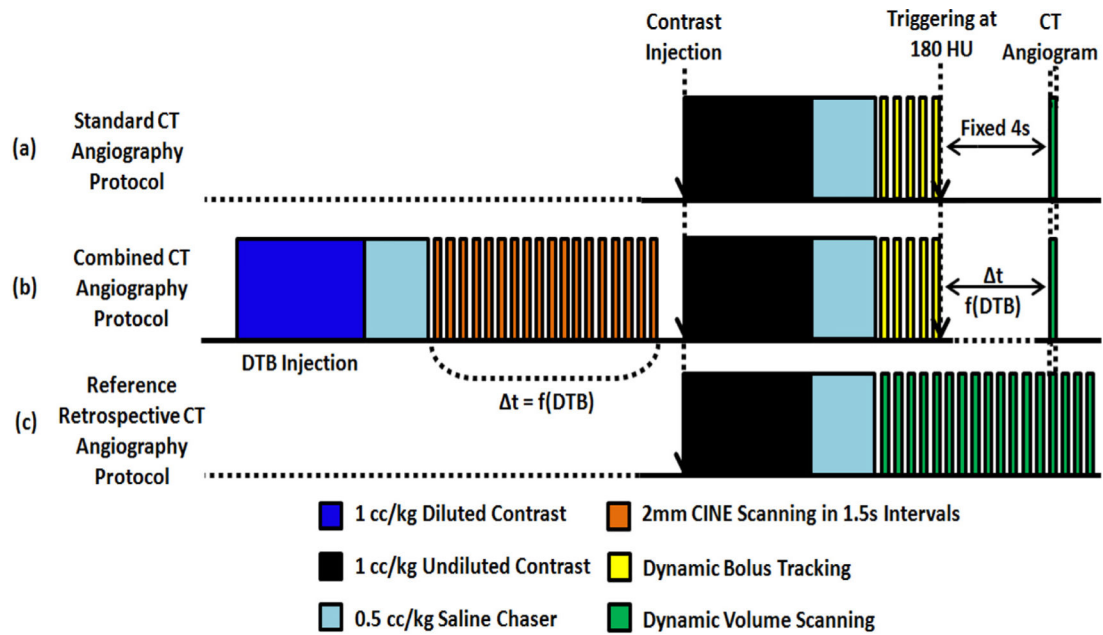


**Figure 3.** Standard, combined, and reference CT angiography acquisition protocol comparison. **(a)** Standard CT angiography protocol, **(b)** combined diluted test bolus (DTB) and CT angiography protocol, and **(c)** reference retrospective CT angiography protocol, where 20 seconds of ECG-gated dynamic imaging was performed to capture peak aortic and coronary enhancement and contrast-to-noise ratio. CT, computed tomography; ECG, electrocardiogram.

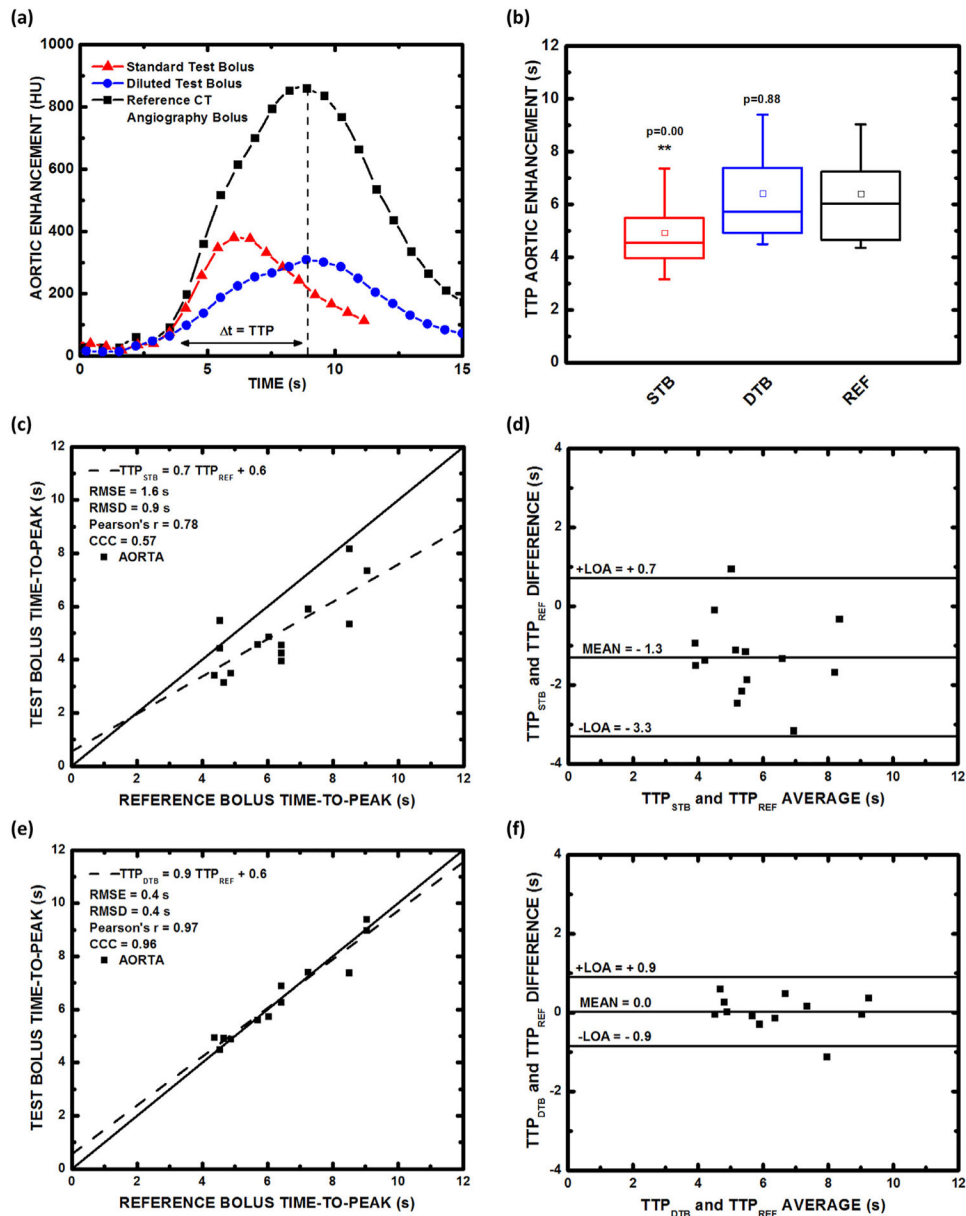


**Figure 4.** Test bolus and reference CT angiography bolus time-to-peak enhancement comparison. **(a)** Bolus time-attenuation curve geometry comparison. **(b)** Bolus time-to-peak (TTP) enhancement box-plot comparison. \*\* indicates  $p < 0.05$ , i.e., a significant time-to-peak difference with the reference CT angiography bolus. **(c)** Regression analysis comparing the standard test bolus time-to-peak data ( $\text{TTP}_{\text{STB}}$ ) to the reference CT angiography bolus time-to-peak data ( $\text{TTP}_{\text{REF}}$ ), with **(d)** corresponding Bland–Altman analysis displayed. **(e)** Regression analysis comparing the diluted test bolus time-to-peak data ( $\text{TTP}_{\text{DTB}}$ ) to the reference CT angiography bolus time-to-peak data ( $\text{TTP}_{\text{REF}}$ ), with **(f)** corresponding Bland–Altman analysis displayed. CCC, Lin's concordance correlation coefficient; CT, computed tomography; DTB, diluted test bolus; LOA, limit of agreement; REF, reference CT

angiography bolus; RMSD, root-mean-square deviation; RMSE, root-mean-square error; STB, standard test bolus.

Author Manuscript

Author Manuscript

Author Manuscript

Author Manuscript

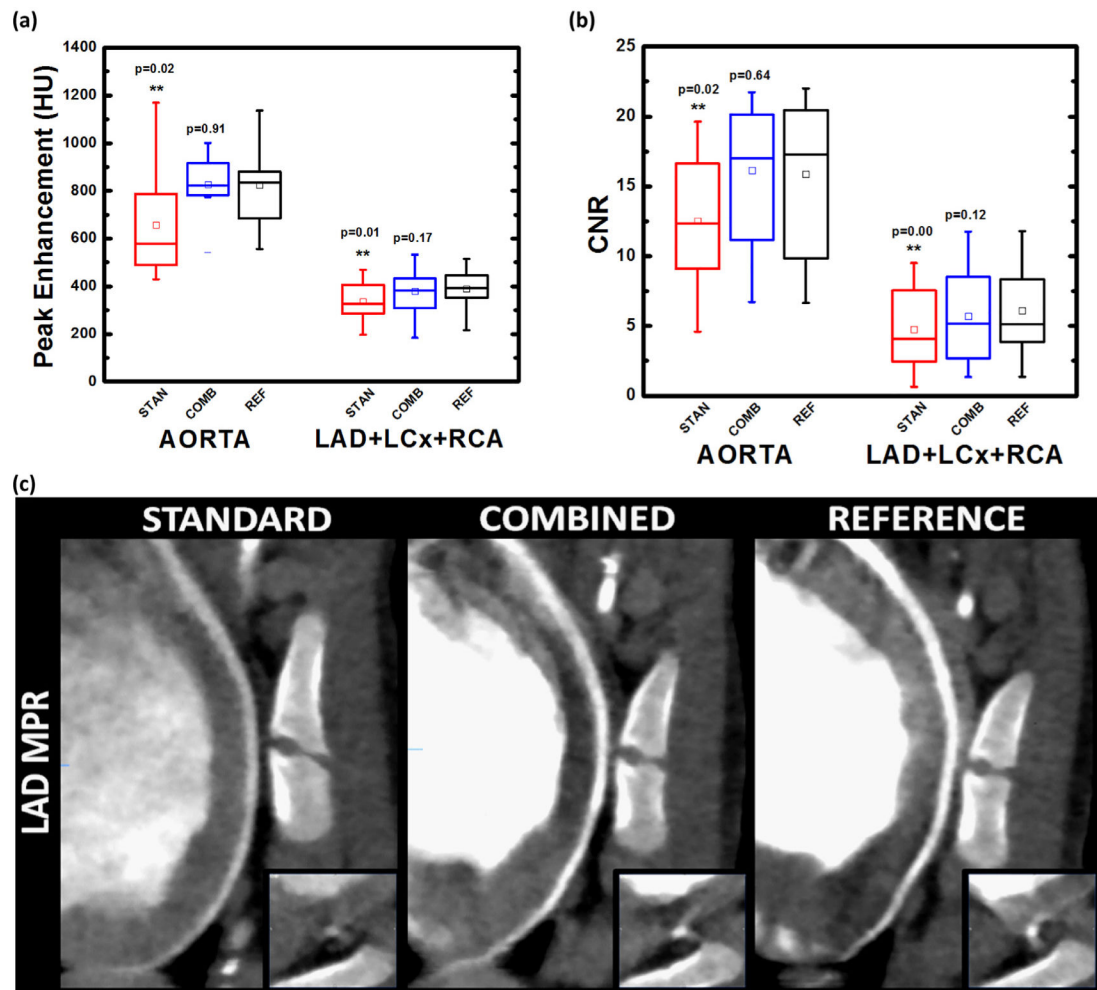


**Figure 5.**

Standard, combined, and reference CT angiography peak enhancement and CNR comparison. **(a)** Aortic and coronary peak enhancement box-plot comparison for the standard and combined CT angiography protocols as compared to a reference retrospective CT angiography protocol. **(b)** Aortic and coronary CNR box-plot comparison for the standard and combined CT angiography protocols as compared to a reference retrospective CT angiography protocol. **(c)** Long-axis and cross-sectional multiplanar reformations (MPRs) of the left anterior descending (LAD) coronary artery for the standard and combined CT angiography protocols as compared to the reference retrospective CT angiography protocol. CNR, contrast-to-noise ratio; CT, computed tomography; HU, Hounsfield units; LAD, left anterior descending; LCx, left circumflex; RCA, right coronary artery. \*\* indicates  $p < 0.05$ , i.e., a significant peak enhancement or CNR difference with the reference retrospective CT angiography data.

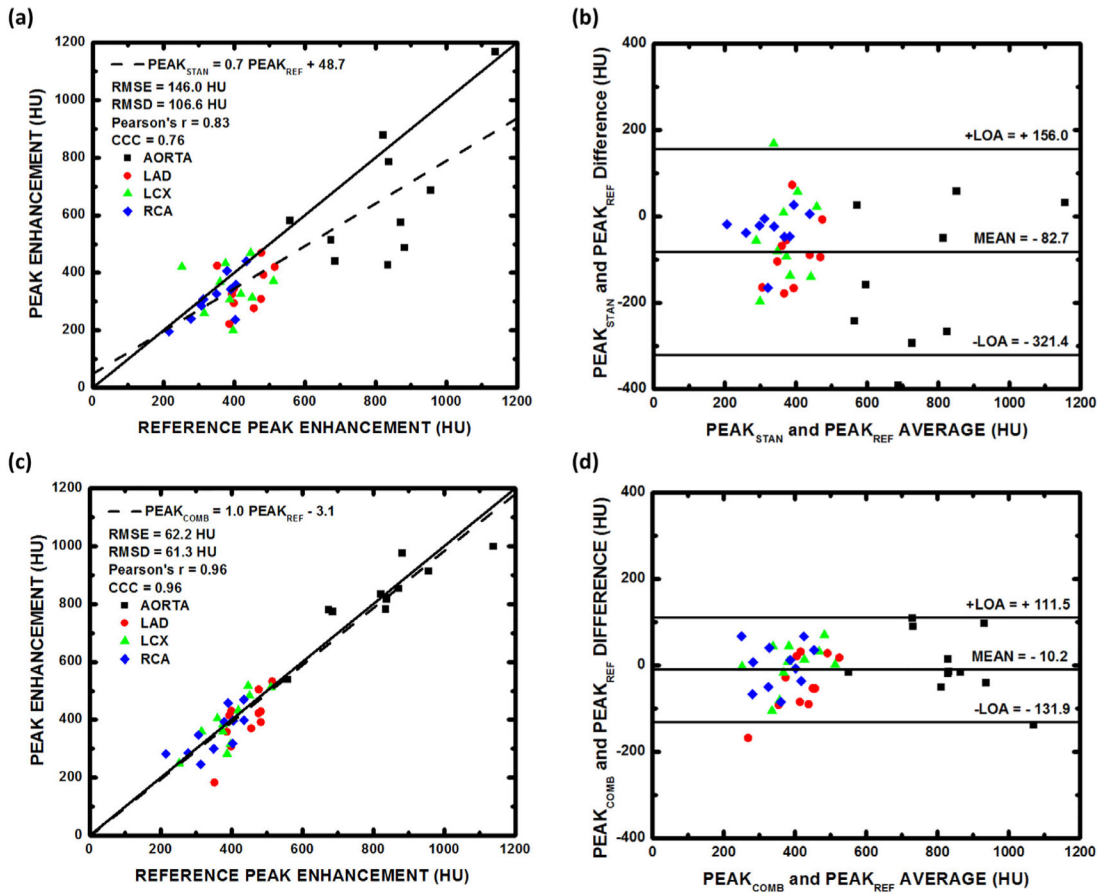


**Figure 6.**

Standard, combined, and reference CT angiography peak enhancement regression analysis. (a) Regression analysis comparing the aortic and coronary peak enhancement data from the standard CT angiography protocol (PEAK<sub>STAN</sub>) to corresponding aortic and coronary peak enhancement data from the reference retrospective CT angiography protocol (PEAK<sub>REF</sub>), with (b) Bland–Altman analysis also displayed. (c) Regression analysis comparing the aortic and coronary peak enhancement data from the combined diluted test bolus and CT angiography protocol (PEAK<sub>COMB</sub>) to corresponding aortic and coronary peak enhancement data from the reference retrospective CT angiography protocol (PEAK<sub>REF</sub>), with (d) Bland–Altman analysis also displayed. CCC, Lin's concordance correlation coefficient; CT, computed tomography; LAD, left anterior descending; LCx, left circumflex; LOA, limit of agreement; RCA, right coronary artery; RMSD, root-mean-square deviation; RMSE, root-mean-square error.

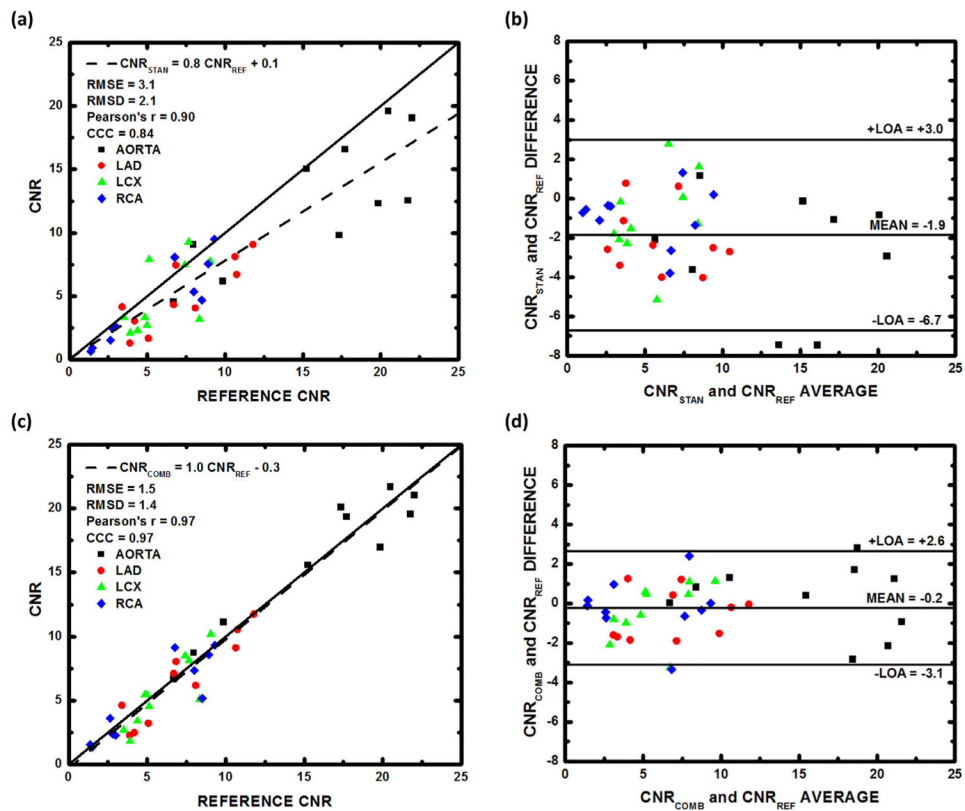


**Figure 7.** Standard, combined, and reference CT angiography CNR regression analysis. **(a)** Regression analysis comparing the aortic and coronary CNR data from the standard CT angiography protocol ( $\text{CNR}_{\text{STAN}}$ ) to corresponding aortic and coronary CNR data from the reference retrospective CT angiography protocol ( $\text{CNR}_{\text{REF}}$ ), with **(b)** Bland–Altman analysis also displayed. **(c)** Regression analysis comparing the aortic and coronary CNR data from a combined diluted test bolus and CT angiography protocol ( $\text{CNR}_{\text{COMB}}$ ) to corresponding aortic and coronary CNR data from the reference retrospective CT angiography protocol ( $\text{CNR}_{\text{REF}}$ ), with **(d)** Bland–Altman analysis also displayed. CCC, Lin's concordance correlation coefficient; CNR, contrast-to-noise ratio; CT, computed tomography; LAD, left anterior descending; LCx, left circumflex; LOA, limit of agreement; RCA, right coronary artery; RMSD, root-mean-square deviation; RMSE, root-mean-square error.

**TABLE 1.** Standard, combined, and reference retrospective CT angiogram peak enhancement and CNR mean comparison

Protocol Standard (N)	CT Angiogram	Reference	<i>p</i> < 0.05
<b>AORTA (10)</b>			
Enhancement (HU)	656.4 ± 232.7	824.4 ± 161.4	0.02**
CNR	12.5 ± 5.2	15.9 ± 5.8	0.02**
<b>LAD (10)</b>			
Enhancement (HU)	348.5 ± 77.3	433.8 ± 53.7	0.01**
CNR	5.0 ± 2.7	7.1 ± 3.1	0.03**
<b>LCx (10)</b>			
Enhancement (HU)	347.3 ± 82.4	391.8 ± 73.2	0.23
CNR	4.9 ± 2.8	5.9 ± 2.0	0.19
<b>RCA (10)</b>			
Enhancement (HU)	314.5 ± 77.1	347.6 ± 68.4	0.07
CNR	4.3 ± 3.2	5.3 ± 3.3	0.07
<b>LAD + LCx + RCA (30)</b>			
Enhancement (HU)	336.8 ± 77.8	391.0 ± 72.7	0.01**
CNR	4.8 ± 2.8	6.1 ± 2.9	0.00**
<b>Combined (N)</b>			
<b>AORTA (10)</b>			
Enhancement (HU)	828.0 ± 122.5	824.4 ± 161.4	0.91
CNR	16.1 ± 5.4	15.9 ± 5.8	0.64
<b>LAD (10)</b>			
Enhancement (HU)	395.5 ± 94.2	433.8 ± 53.7	0.05
CNR	6.6 ± 3.4	7.1 ± 3.1	0.18
<b>LCx (10)</b>			
Enhancement (HU)	391.1 ± 89.8	391.8 ± 73.1	0.96
CNR	5.5 ± 2.7	5.9 ± 2.0	0.41
<b>RCA (10)</b>			

Protocol	CT Angiogram	Reference	$p < 0.05$
<i>Enhancement (HU)</i>	354.2 ± 74.4	347.6 ± 68.4	0.93
<i>CNR</i>	5.1 ± 3.3	5.3 ± 3.3	0.67
<b>LAD + LCx + RCA (30)</b>			
<i>Enhancement (HU)</i>	380.3 ± 85.9	391.0 ± 72.7	0.17
<i>CNR</i>	5.7 ± 3.1	6.11 ± 2.9	0.12

Unless otherwise stated, all peak enhancement and CNR data are mean ± SD.

CT, computed tomography; CNR, contrast-to-noise ratio; DTB, diluted test bolus; HU, Hounsfield units; LAD, left anterior descending; LCx, left circumflex; N, number of measurements; RCA, right coronary artery.

\*\*  $p < 0.05$ , i.e., a significant peak enhancement or CNR difference as compared to the reference.

**TABLE 2.** Standard, combined, and reference retrospective CT angiogram peak enhancement and CNR regression analysis

Protocol Standard (N)	Slope	Intercept	r	CCC	RMSE	RMSD
<b>AORTA (10)</b>						
Enhancement (HU)	0.9 [0.1, 1.8]	-119.7 [-866.1, 626.6]	0.65 [0.04, 0.91]	0.45 [-0.25, 0.84]	237.2	167.2
CNR	0.7 [0.3, 1.2]	1.2 [-6.2, 8.6]	0.80 [0.34, 0.95]	0.67 [0.07, 0.91]	4.7	3.0
<b>LAD (10)</b>						
Enhancement (HU)	0.5 [-0.6, 1.6]	136.6 [-345.7, 618.8]	0.34 [-0.37, 0.79]	0.17 [-0.51, 0.72]	112.7	69.0
CNR	0.7 [0.3, 1.1]	-0.2 [-3.3, 2.8]	0.83 [0.43, 0.96]	0.65 [0.04, 0.91]	2.7	1.4
<b>LCx (10)</b>						
Enhancement (HU)	0.0 [-0.9, 0.9]	340.5 [-24.6, 705.7]	0.02 [-0.62, 0.64]	0.01 [-0.62, 0.64]	112.9	78.2
CNR	0.9 [0.0, 1.8]	-0.2 [-5.8, 5.4]	0.62 [-0.02, 0.90]	0.54 [-0.13, 0.87]	2.3	2.1
<b>RCA (10)</b>						
Enhancement (HU)	0.9 [0.2, 1.5]	19.9 [-194.4, 234.2]	0.75 [0.23, 0.94]	0.68 [-0.08, 0.92]	59.3	48.2
CNR	0.9 [0.5, 1.2]	-0.3 [-2.4, 1.8]	0.90 [0.63, 0.98]	0.87 [0.52, 0.97]	1.7	1.3
<b>LAD + LCx + RCA (30)</b>						
Enhancement (HU)	0.4 [0.0, 0.8]	173.8 [22.0, 325.5]	0.39 [0.03, 0.66]	0.31 [-0.06, 0.60]	98.3	70.5
CNR	0.8 [0.6, 1.0]	0.0 [-1.6, 1.6]	0.79 [0.60, 0.90]	0.71 [0.47, 0.85]	2.3	1.7
<b>Combined (N)</b>						
<b>AORTA (10)</b>						
Enhancement (HU)	0.7 [0.4, 1.0]	245.7 [7.8, 483.5]	0.88 [0.60, 0.97]	0.86 [0.54, 0.96]	69.8	59.9
CNR	0.9 [0.7, 1.1]	2.0 [-2.0, 5.9]	0.95 [0.81, 0.99]	0.95 [0.80, 0.99]	1.7	1.6
<b>LAD (10)</b>						
Enhancement (HU)	1.4 [0.5, 2.2]	-196.8 [-580.3, 186.6]	0.76 [0.30, 0.93]	0.56 [-0.06, 0.87]	74.4	58.3
CNR	1.0 [0.7, 1.3]	-0.6 [-3.2, 1.9]	0.93 [0.71, 0.98]	0.91 [0.65, 0.98]	1.3	1.2
<b>LCx (10)</b>						
Enhancement (HU)	1.0 [0.5, 1.6]	-15.9 [-242.8, 211.1]	0.81 [0.41, 0.95]	0.78 [0.34, 0.94]	50.5	50.5
CNR	1.2 [0.6, 1.7]	-1.3 [-4.8, 2.3]	0.85 [0.48, 0.96]	0.81 [0.36, 0.95]	1.4	1.3
<b>RCA (10)</b>						
Enhancement (HU)	0.8 [0.2, 1.3]	75.8 [-120.5, 272.1]	0.74 [0.25, 0.93]	0.73 [0.24, 0.93]	50.2	48.0

Protocol	Slope	Intercept	<i>r</i>	CCC	RMSE	RMSD
CNR	0.9 [0.6, 1.2]	0.4 [-1.8, 2.5]	0.90 [0.63, 0.98]	0.90 [0.63, 0.98]	1.4	1.3
<b>LAD + LCx + RCA (30)</b>						
Enhancement (HU)	0.9 [0.6, 1.1]	30.5 [-88.8, 149.7]	0.74 [0.53, 0.86]	0.71 [0.49, 0.85]	59.5	57.1
CNR	1.0 [0.8, 1.2]	-0.2 [-1.4, 1.0]	0.90 [0.80, 0.95]	0.89 [0.78, 0.95]	1.4	1.3

Brackets indicate 95% confidence intervals.

CCC, Lin's concordance correlation coefficient; CNR, contrast-to-noise ratio; CT, computed tomography; DTB, diluted test bolus; HU, Hounsfield units; LAD, left anterior descending; LCx, left circumflex; *N*, number of measurements; *r*, Pearson's correlation coefficient; RCA, right coronary artery; RMSD, root-mean-square deviation; RMSE, root-mean-square error.